

# Invariant Representation and Hierarchical Network for Inspection of Nuts from X-ray Images \*

A. Sim and B. Parvin

Information and Computing Sciences Division  
Lawrence Berkeley National Laboratory  
Berkeley, CA 94720

P. Keagy

Western Regional Research Center  
U.S. Dept. of Agriculture  
Albany, CA 94710

## Abstract

An X-ray based system for the inspection of pistachio nuts and wheat kernels for internal insect infestation is presented. The novelty of this system is two-fold. First, we construct an invariant representation of infested nuts from X-ray images that is rich, robust, and compact. Insect infestation creates a tunnel, in the X-ray image, with reduced density of the natural material. The tunneling effect is encoded by linking troughs on the image and constructing a joint curvature-proximity distribution table for each nut. The latter step is designed to accentuate separation of those tunneling effects that are due to the natural structure of the nut. Second, since the representation is sparse, we partition the joint distribution table into several regions, where each region is used independently to train a backpropagation (BP) network. The outputs of these subnets are then collectively trained with another BP network. We show that the resulting hierarchical network has the advantage of reduced dimensionality while maintaining a performance similar to the standard BP network.

## 1 Introduction

We present a system that has been developed for inspection of pistachio nuts and wheat kernels viewed with an X-ray sensor. The X-ray device reveals internal defects that cannot be otherwise detected by external evidences in the visible domain. Presently, pistachio nuts are inspected for external damages, and a sample of wheat kernels are X-rayed for manual inspection at the mill. In the case of pistachio nut, we are interested in aflatoxin contamination<sup>1</sup> [15]. However, there is a strong correlation between contamination and insect infestation. And in the case of wheat kernels, we are interested in rejecting those wheat kernels that are infested with maize weevils.

The main novelty of this paper is two fold: First, we derive an *invariant* representation that captures pertinent information on infested as well as non-infested nuts; second, we show that by partitioning this invariant representation, a classifier with reduced dimensionality can be constructed. From a geometric perspective, infestation can be character-

ized by a dark tunneling appearance in the X-ray image. The tunnel corresponds to the reduced density of the natural content of the nut and to the replacement of that content by a cocoon, insect debris, and air, which have lower X-ray absorption properties. The construction of an invariant representation is complicated by the fact that the tunnel can occur at any spatial location and direction. In case of pistachio nuts, some air gaps are due to natural separations between the two halves (cotyledons) of the nut meat. And in the case of the wheat kernel, the density of the kernel is reduced near its medial axis.

For pistachio nuts, these natural features may be visible depending upon its resting position. However, the natural separations are generally accentuated by higher contrast than those that are caused by infestation. In this context, our invariant representation first encodes the tunnels and their magnitude, and then parametrizes this representation with respect to location and orientation. Tunnels can be represented in terms of local positive curvature maxima; these local maxima are then linked to form long curve segments. The invariant and compact representation of these curve segments, with respect to rotation and translation, is then encoded by constructing the distribution of local curvature maxima as a function of distance to the outer boundary of the nut. This distribution is a two dimensional joint histogram with the necessary invariant properties.

The second aspect of our work is in the design of the classifier, which is based on the backpropagation network. In general, the corresponding representation for infested nuts is sparse; and our classifier utilizes this property to partition the histogram into several regions, training a network for each region independently, and combining these subnets in a hierarchical fashion. The main benefit is that a classifier with reduced dimensionality (number of weights) than a standard backpropagation network can be obtained.

In the next section, a brief summary of the image acquisition system is given. Then in sections 3 and 4, we outline the details of the invariant representation and classification. In each section, we present the intermediate result of our system followed by examples. Representation of pistachio nuts is a far more complex and interesting problem than the wheat kernels. The paper concludes in section 5 with a summary and a description of future efforts.

\*Research was supported by a grant from the U.S. Dept. of Agriculture, under contract number 6053253132.

<sup>1</sup>Aflatoxin is a natural carcinogenic compound, and its concentration is limited by the U.S. and European regulatory agencies.

## 2 Images

In this section, the details of the imaging system for pistachio nuts are covered. The wheat kernels are imaged at higher resolution and a description can be found in [8].

The X-ray images of clean and infested pistachios are captured on photographic film. Nuts from each process stream (Table 2) are individually arrayed on clear adhesive contact paper in one of three orientations (suture plane parallel, perpendicular or at an angle to the film plane) and X-rayed<sup>2</sup>. Films are handled in the dark and exposed without film holders. Twelve bit digital images are obtained from the films at a resolution<sup>3</sup> of  $(0.125mm)^2/pixel$ . The X-rayed nuts are then opened to determine the presence of insect damage. An image of a clean nut will have the following characteristics: a bright area representing the nut meat, surrounded by a small dark gap between the nut meat and the shell, and a little brighter nut shell outside the kernel. Often there is a dark gap between the two halves of the kernel. The dark areas generally have sharp edges. An insect-infested nut has additional dark areas in the kernel which have been caused by insect bites or tunneling. Figures 1 and 2 show representative images of pistachio and wheat kernels respectively.



Figure 1: X-ray images of pistachios: (a) & (b) clean and (c) & (d) infested

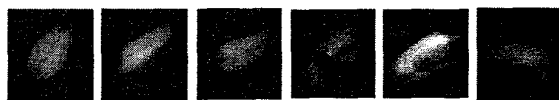


Figure 2: X-ray images of wheats: (a), (b) & (c) clean and (d), (e) & (f) infested

## 3 Invariant Representation

In this section, we present the details of the invariant representation for the pistachio nuts. The representation of wheat kernels is a slightly simpler problem, and the result should be easily extendable. An ideal representation should capture meaningful features with maximum compactness for effective classification. In this context, the low level representations should be rich, stable, and invariant to the rotation and translation of the object in the image plane as well as in the 3-D space. Compactness in representation can be achieved by encoding the

<sup>2</sup>90 seconds at 25 keV [0.25 mm Be window] with a Faxitron series X-ray system 4380N, Hewlett Packard, McMinnville, OR; Industrex B film, Eastman Kodak, Rochester, NY

<sup>3</sup>using a Lumiscan 200 film scanner, Lumisys, Sunnyvale, CA

low level features so that similar structures at different spatial locations have the same representation. For example, a cocoon on the left or right side of the nut should be represented identically. In our system, the ideal properties of the low level features are captured by computing the surface curvature at each pixel position. Curvature measurements are invariant to translation and rotation, and their positive local maxima identify the positions of troughs. However, other maxima may also be the results of natural surface properties of the pistachio nut such as the split cotyledon. Still, we assert that curvature maxima on the natural surface have higher magnitude, statistically, at a given distance from the nut boundary when these are compared to those curvature maxima, obtained at the identical distance from the nut boundary, that are due to the infestation. Compactness is achieved by parametrizing curvature features as a function of their distance from the boundary of the nut. This parametrization is constructed as a two dimensional histogram that encodes the curvature-distance joint distribution. We suggest that this histogram corresponds to the signature, or a finger print, that can characterize an infested or clean nut, and we present results to that effect. The system architecture is shown in figure 3, and the details of the above computational steps are outlined below.

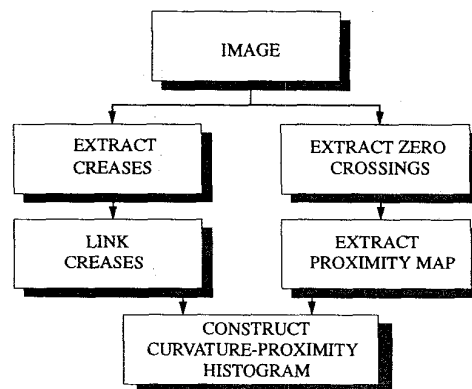


Figure 3: Processing steps

The tunnels are localized by grouping local positive curvature maxima, where curvature corresponds to the differential surface properties of the local intensity distribution for the projected image of the tunnel. Curvature is computed from the first and second fundamental forms. These forms uniquely determine certain local invariant quantities of a 3-D surface, where invariance is expressed in terms of translation, rotation, and scaling for X-ray images. Faux and Pratt [3] expressed the first and second fundamental forms in parametric space. However, from a computational perspective, it is desirable to express these forms in Cartesian space. Let a point on the surface be defined as  $P = x\vec{i} + y\vec{j} + z\vec{k}$ ; then the first and the second

fundamental forms are computed to be:

$$G = \begin{bmatrix} 1 + \left(\frac{\partial z}{\partial x}\right)^2 & \frac{\partial z}{\partial x} \frac{\partial z}{\partial y} \\ \frac{\partial z}{\partial x} \frac{\partial z}{\partial y} & 1 + \left(\frac{\partial z}{\partial y}\right)^2 \end{bmatrix} \quad (1)$$

$$D = \begin{bmatrix} \frac{\partial^2 z}{\partial x^2} & \frac{\partial^2 z}{\partial x \partial y} \\ \frac{\partial^2 z}{\partial x \partial y} & \frac{\partial^2 z}{\partial y^2} \end{bmatrix} \quad (2)$$

The normal curvature of a surface is the curvature of the intersecting curve between the surface and the plane containing the surface normal and tangent vector to the curve. The directions in which the normal curvature becomes maximum or minimum are called principal directions corresponding to the principal curvatures. The normal curvature is defined as [3]:

$$K_n = \frac{\dot{X}^T D \dot{X}}{\dot{X}^T G \dot{X}} \quad \text{where } \dot{X}^T = \left[ \frac{\partial z}{\partial x} \quad \frac{\partial z}{\partial y} \right] \quad (3)$$

Through elimination and the solution of a pair of simultaneous equations, the following quadratic equation is obtained, where the roots of this equation correspond to maximum and minimum principal curvatures.

$$\begin{aligned} & (g_{11}g_{22} - g_{12}g_{21})k_n^2 \\ & - (g_{11}d_{22} + d_{11}g_{22} - 2g_{12}d_{12})k_n \\ & + (d_{11}d_{22} - d_{12}d_{21}) = 0 \end{aligned} \quad (4)$$

Figure 4 shows the curvature features corresponding to the images shown in figure 1, and figure 5 shows the curvature features corresponding to the images shown in figure 2. On these images, white pixels correspond to troughs (positive curvature maxima) and black pixels to ridges (negative curvature maxima) respectively.

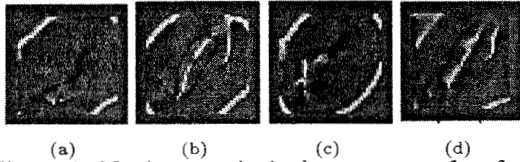


Figure 4: Maximum principal curvatures of surface intensity for pistachios: (a) & (b) clean and (c) & (d) infested

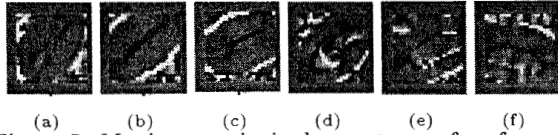


Figure 5: Maximum principal curvatures of surface intensity for wheats: (a), (b) & (c) clean and (d), (e) & (f) infested

Once local curvature maxima are determined, they are linked together and long segments are constructed. The steps leading to the extraction of trough segments are enumerated below.

1. Smooth the original image with a Gaussian kernel,
2. Compute the curvatures at each pixel on the smooth image,
3. Threshold the curvature image for troughs,
4. Thin the thresholded image using the non-maximal suppression [2] method. The idea is to keep only the troughs whose maximum curvature is the local maximum, and
5. Link the thinned troughs using a hysteresis [2] method. The hysteresis linking method consists of a high and a low threshold. All points above the high threshold are marked as trough points, and similarly, those points below the low threshold are marked as non-trough points. The points between the low and high thresholds can only be traversed from those troughs that are marked by the high threshold.

The result of linking troughs for pistachios and wheats are shown in figure 6 and figure 7. These images are computed with high threshold of 0.99, low threshold of 0.89, and the kernel size of 1.5 for Gaussian smoothing for pistachios, and for wheats, the kernel size of 1.0 is used. These parameters are found to be experimentally appropriate for the nut size, and the expected size of the cocoon that is generated through infestation.

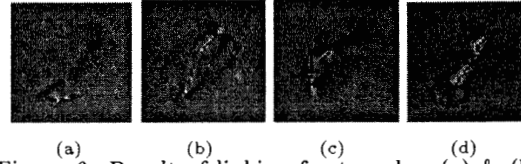


Figure 6: Result of linking for troughs: (a) & (b) clean and (c) & (d) infested pistachios

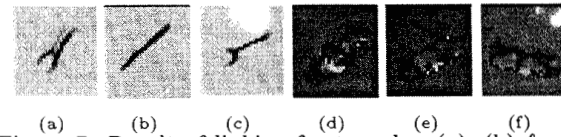


Figure 7: Result of linking for troughs: (a), (b) & (c) clean and (d), (e) & (f) infested wheats

In the next step of the computational process, we compute the distance from each trough point to the boundary of the nut. This is accomplished by first extracting the boundary of the nut with the zero-crossings of the Difference of Gaussian (DoG) filter, and then computing the chamfer image. The chamfer image generates a distance map from edges. The map has a zero value on the edge and increases monotonically from the edge. Figure 8 shows the chamfer images obtained from the boundaries of the pistachios nuts shown in figure 1. Once the proximity map is computed, the two dimensional joint distribution of the curvature-distance table is constructed. Figure 9 shows the cumulative curvature-distance joint histogram for a clean and an infested pistachio, corresponding to the second and

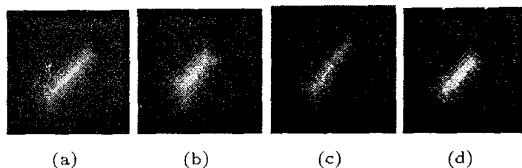


Figure 8: Chamfer images of boundaries of the pistachios: (a) & (b) clean and (c) & (d) infested

the fourth images from example respectively. In

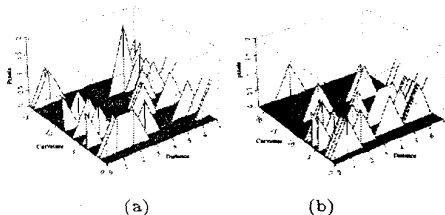


Figure 9: Joint histograms of curvature and proximity values: (a) clean nut and (b) infested nut

figure 9, the distribution indicates that high curvature activities are more localized, at a given distance from the boundary, for clean pistachios than infested pistachios.

In the next section, we show that the joint distribution has the necessary information content to identify the infested nuts in the population.

#### 4 Classification

In the design of the classifier, we experimented with several indexing schemes, such as Bidirectional Associative Memory [9] and backpropagation neural network paradigms. The latter consistently produced more favorable results. This is in part due to the large variation in pattern structure and the presence of similar patterns among clean and infested pistachios. The basis for classification is the joint distribution of the curvature-distance table. The curvature values range from 0 to 7.5, and are partitioned into 16 groups, with the distance values ranging from 0 to 9, partitioned into 10 groups. The table is further quantized, as shown in table 1, to reduce the size of the network used for classifying based on the joint distribution and consequently, the size of the training set. The training is based on the backpropagation algorithm. We have experimented with two strategies for further refinement of the classifier design. The first one is the standard backpropagation technique for training a network from a population. In the second approach, we partition the joint distribution table into several regions, where each region is used independently to train a network. These subnets are then trained with another backpropagation network. The backpropagation (BP) algorithm is a supervised training technique. In the rest of this section, we first evaluate the performance of a standard BP network, then compare its results with the hierarchical one.

	Curvatures	Distances		
		1 2 3 4	5 6 7	8 9 10
1 2 3 4	group 1	group 2	group 3	
5 6 7 8	group 4	group 5	group 6	
9 10 11 12	group 7	group 8	group 9	
13 14 15 16	group 10	group 11	group 12	

Table 1: Quantization of joint histogram of the curvature and proximity values

In the standard implementation of the backpropagation algorithm, we use a three layer network and create a sequential array of the joint distribution table as the input to this network. The learning rate and the momentum factor are set at 0.1 and 0.9 respectively. These parameters are selected to maintain a balance between achieving fast convergence and arriving at the desirable local minima. The samples are arranged in different trays, and manually identified as clean or defective nuts. Table 2 tabulates the types of defective pistachio nuts in these trays. The training set consists of a sample of 80 clean and infested pistachio nuts. The clean and infested pistachio nuts are randomly selected from trays M and Q respectively. We construct three sets

Product Stream	% of Total Product	Aflatoxin NG/GM	Aflatoxin % of Crop Toxin	Insects per 100 nuts
M	31.06	0	0	0
Q	0.89	89	37	44
A	10.91	1.4	7	2
D	0.13	91	9	9
I	0.53	97	24	13

Tray	Description
M	Good large nuts
Q	Nuts manually removed
A	Nuts with stained shells
D	Lightly stained nuts
I	Small nuts

Table 2: Processing Stream Information of testing data for pistachios. The first and second set have 98 and 100 samples from trays M and Q, respectively. The third set has 452 samples from all the trays. For the classification for wheat kernels, 742 random samples are drawn for training, and another 744 random samples are selected for testing. All samples are selected randomly without replacement, and none of the testing samples are included in the training set. The classification results for pistachios for the backpropagation network with various input size and nodes in the hidden layer are shown in table 3. The poor performance of the third set is due to the presence of other categories of pistachio nuts, as listed in table 2, that in addition of being infested or clean, they may have other defects as well. In a usual agricultural setting, the inspection of pistachio nuts is a multi-stage process, where at each stage, different types of defects or nut grades are inspected. For example, nuts with external defects such as stained shells, are removed by a different inspection system all together. The third set of data was constructed as an experiment to test

if the multi-stage inspection and grading process can be reduced into one single stage. Our result indicate that a two class image-based recognition system is not capable of discriminating the nuts effectively. For wheats, the classification results with the standard backpropagation network are shown in table 4. The table 4 also shows specific classification results for each infestation category.

Other researchers have explored hierarchical networks for machine vision applications [14] as well. However, our implementation does not use shared weights, nor use more than one hidden layer, and it treats the output of each subnet as a probability measure. Furthermore, the representation used by other researchers is at the pixel level, and no invariant properties of image features are exploited. In our implementation, we divide the joint distribution of histogram into four or six regions (the number of regions is arbitrary). Each region is then used independently to train a BP network. The results of these subnets are then used as input for the next BP network, as shown in figure 10. The classification results for pistachios with various network sizes are tabulated in table 5. Also, the classification results for wheats with the hierarchical backpropagation network are shown in table 6, along with the results for each infestation category. The re-

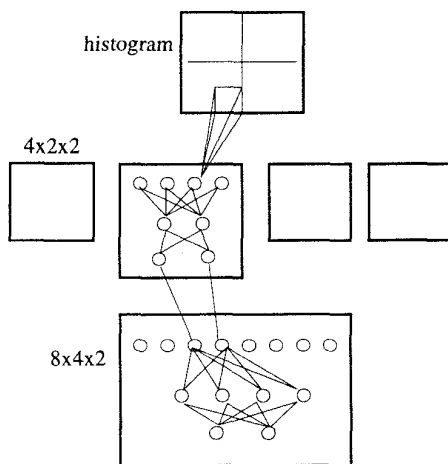


Figure 10: Hierarchical Backpropagation Networks

sult from our hierarchical network approach shows a similar performance to the standard backpropagation network, while reducing the dimensionality. As an example, from the classification results for pistachios, the fourth row (20x5x2, 110 weights) from table 3 and the fifth row (L: 4x2x2, H: 8x4x2, 88 weights) from table 5 indicates that the hierarchical BP network with similar performance to the standard BP network has the reduced dimensionality. The  $\chi^2$  test on this example confirms the result as the  $\chi^2$  value 6.3185 with 6 degrees of freedom. The reduced dimensionality of the network has the benefit of improved convergence time and a reduction

NODES	WEIGHTS	NTRS	NTEs	TPF	FPF
24x12x2	312	80	98	0.7959	0.3285
			100	0.9200	0.2200
			452	0.8214	0.4441
24x6x2	168	80	98	0.8776	0.4082
			100	0.9400	0.2400
			452	0.8571	0.4647
20x10x2	220	80	98	0.7347	0.3265
			100	0.8000	0.1800
			452	0.7411	0.3735
20x5x2	110	80	98	0.7959	0.3081
			100	0.8200	0.2400
			452	0.8125	0.4324
16x4x2	72	80	98	0.7755	0.3469
			100	0.9000	0.2800
			452	0.8482	0.4412
12x4x2	56	80	98	0.6327	0.3673
			100	0.7200	0.3000
			452	0.6429	0.4206
6x3x2	24	80	98	0.3388	0.7755
			100	0.3800	0.7000
			452	0.3018	0.7706

NODES: number of nodes in the networks  
 WEIGHTS: number of computed weights  
 NTRS: number of training samples  
 NTEs: number of testing samples  
 TPF: true positive fraction as the percent of infested nuts actually detected  
 FPF: false positive fraction as the percent of clean nuts mistakenly identified as infested

Table 3: Performance of standard backpropagation networks on pistachio nuts with varying number of nodes and hidden layers

in the number of required training samples.

## 5 Conclusion

An inspection system for the classification of infested and clean pistachio nuts and wheat kernels is presented. The novelty of our approach lies in the compact and invariant representation of the image features for recognition. The invariance was expressed in terms of curvature-proximity joint distribution function. Furthermore, we showed that by partitioning the sparse input array and hierarchical organization of the BP network, we could reduce the dimensionality in the network significantly, without the loss of accuracy. This result leads us to conclude that we need fewer of training samples, and that we can reduce the cost of the inspection of pistachios. We believe that this architecture can be used to inspect other varieties of nuts as well, which is the focus of our current effort.

## References

- [1] R. Anan, K. Mehrotra, C. K. Mohan, and S. Ranka. Analyzing images containing multiple sparse patterns with neural networks. *Pattern Recognition*, 26(11):1717-1724, 1993.
- [2] J. F. Canny. A computational approach to edge detection. *IEEE Transactions on Pattern Analysis and Machine Intelligence*, 8(6):679-698, November 1986.
- [3] I. D. Faux and M. J. Pratt. *Computational geometry for design and manufacture*. Ellis Horwood series in mathematics and its applications. Halsted Press, New York, 1979.
- [4] J. M. Gauch and S. M. Pizer. Multiresolution analysis of ridges and valleys in grey-scale images. *IEEE Transactions on Pattern Analysis and Machine Intelligence*, 15(6):635-646, June 1993.
- [5] R. C. Gonzalez and R. E. Woods. *Digital image processing*. Addison-Wesley, Reading, Mass., 1993.
- [6] P. M. Keagy, B. Parvin, and T. F. Schatzki. Machine recognition of naval orange worm damage in x-ray images of pistachio nuts. *Optics in Agriculture, Forestry and Biological*, SPIE Proceedings 2345, 1994.

NODES	WEIGHTS	NTRS	NTES	TPF	FPF
24x6x2	168	742	744	0.7946	0.0904
			Days	TPF	
			45	0.9286	
			42	0.9286	
			38	0.8929	
			35	0.8571	
			31	0.7857	
			28	0.8571	
			24	0.6071	
			21	0.5000	
20x5x2	110	742	744	0.7946	0.0712
			Days	TPF	
			45	0.8929	
			42	0.9286	
			38	0.9286	
			35	0.8929	
			31	0.8214	
			28	0.8929	
			24	0.5357	
			21	0.4643	
16x4x2	72	742	744	0.8125	0.0750
			Days	TPF	
			45	0.9286	
			42	0.9643	
			38	0.8571	
			35	0.8929	
			31	0.9286	
			28	0.8571	
			24	0.5357	
			21	0.5357	

NODES: number of nodes in the networks  
 WEIGHTS: number of computed weights  
 NTRS: number of training samples  
 NTES: number of testing samples  
 L: lower subnetwork  
 H: upper network  
 TPF: true positive fraction as the percent of infested nuts actually detected  
 FPF: false positive fraction as the percent of clean nuts mistakenly identified as infested  
 Days: the age of infested wheats

Table 4: Performance of standard backpropagation networks on wheat kernels with varying number of nodes and hidden layers

NODES	WEIGHTS	NTRS	NTES	TPF	FPF
L 6x4x2 H 12x8x2	304	80	98	0.7143	0.2857
			100	0.8400	0.2600
			452	0.6786	0.3765
L 6x3x2 H 12x4x2	200	80	98	0.8163	0.3673
			100	0.8600	0.2400
			452	0.7589	0.4471
L 6x2x2 H 12x4x2	152	80	98	0.8367	0.3265
			100	0.8600	0.2000
			452	0.6607	0.4706
L 4x3x2 H 8x4x2	112	80	98	0.7959	0.3673
			100	0.7800	0.2600
			452	0.7321	0.4559
L 4x2x2 H 8x4x2	88	80	98	0.8163	0.3673
			100	0.8400	0.2600
			452	0.7054	0.3765
L 4x1x2 H 8x2x2	44	80	98	0.7143	0.2245
			100	0.7000	0.2400
			452	0.5893	0.3029
L 4x1x2 H 8x1x2	34	80	98	0.7143	0.2449
			100	0.7400	0.2600
			452	0.6250	0.3794

NODES: number of nodes in the networks  
 WEIGHTS: number of computed weights  
 NTRS: number of training samples  
 NTES: number of testing samples  
 L: lower subnetwork  
 H: upper network  
 TPF: true positive fraction as the percent of infested nuts actually detected  
 FPF: false positive fraction as the percent of clean nuts mistakenly identified as infested

Table 5: Performance of hierarchical backpropagation networks on pistachio nuts with subnet size of 4 and 6 with varying number of nodes and hidden layers

NODES	WEIGHTS	NTRS	NTES	TPF	FPF
L 6x2x2 H 12x4x2	152	742	744	0.8080	0.0808
			Days	TPF	
			45	0.9286	
			42	0.9643	
			38	0.8571	
			35	0.8214	
			31	0.8571	
			28	0.9286	
			24	0.6429	
			21	0.4643	
L 4x3x2 H 8x4x2	112	742	744	0.7634	0.0577
			Days	TPF	
			45	0.8929	
			42	0.9286	
			38	0.8929	
			35	0.8214	
			31	0.8571	
			28	0.8571	
			24	0.4643	
			21	0.4286	
L 4x2x2 H 8x4x2	88	742	744	0.7768	0.0769
			Days	TPF	
			45	0.9286	
			42	0.9286	
			38	0.7857	
			35	0.7857	
			31	0.8929	
			28	0.8214	
			24	0.6071	
			21	0.4643	

NODES: number of nodes in the networks  
 WEIGHTS: number of computed weights  
 NTRS: number of training samples  
 NTES: number of testing samples  
 L: lower subnetwork  
 H: upper network  
 TPF: true positive fraction as the percent of infested nuts actually detected  
 FPF: false positive fraction as the percent of clean nuts mistakenly identified as infested  
 Days: the age of infested wheats

Table 6: Performance of hierarchical backpropagation networks on wheat kernels with subnet size of 4 and 6 with varying number of nodes and hidden layers

- P. M. Keagy and T. F. Schatzki. Effect of image resolution on insect detection in wheat radiographs. *Cereal Chemistry*, 68(4):339-343, 1991.
- P. M. Keagy and T. F. Schatzki. Machine recognition of weevil damage in wheat radiographs. *Cereal Chemistry*, 70(6):696-700, 1993.
- B. Kosko. *Neural networks and fuzzy systems: a dynamical systems approach to machine intelligence*. Prentice Hall, Englewood Cliffs, NJ, 1992.
- L. Lam, S. Lee, and C. Y. Suen. Thinning methodologies - a comprehensive survey. *IEEE Transactions on Pattern Analysis and Machine Intelligence*, 14(9):869-885, September 1992.
- S. Lu and A. Szeto. Hierarchical artificial neural networks for edge enhancement. *Pattern Recognition*, 26(8):1149-1163, 1993.
- W. K. Pratt. *Digital image processing*. Wiley, New York, N.Y., 1991.
- T. F. Schatzki and P. M. Keagy. Effect of image size and contrast on the recognition of insects in radiograms. *Optics in Agriculture*, SPIE Proceedings 1379:182-188, 1991.
- S. A. Solla and Y. le Cun. Constrained neural networks for pattern recognition. In P. Antognetti and V. Milutinovic, editors. *Neural networks: concepts, applications, and implementations*. Prentice Hall advanced reference series, pages 142-161. Prentice Hall, Englewood Cliffs, N.J., 1991.
- N. F. Sommer, J. R. Buchanan, and R. J. Fortlage. Relation of early splitting and tattering of pistachio nuts to aflatoxin in the orchard. *Phytopathology*, 76:692-694, 1986.